

CT Scan Analysis of Liver Lesion Segmentation with U-Net-ResNeXt Architecture

Sonwane Suchitra Shivaji Rao¹, Dr. K Gangadhara Rao^{2*}

^{1,2*}Computer Science, Acharya Nagarjuna University, Nagarjuna Nagar, Guntur, 522510, AP, India.

***Corresponding author:**

Email ID: gharde.suchitra@gmail.com; Email ID: kancherla123@gmail.com

Cite this paper as: Sonwane Suchitra Shivaji Rao, Dr. K Gangadhara Rao, (2025) CT Scan Analysis of Liver Lesion Segmentation with U-Net-ResNeXt Architecture. *Journal of Neonatal Surgery*, 14 (30s), 877-886.

ABSTRACT

Image segmentation in the medical field has resulted in detection of various tumors like brain, intestine, skin and liver etc. Segmentation can be performed manually, but the process may be time consuming and the outcomes might be faulty. Hence, automatic liver tumor segmentation helps to detect heterogeneous tumor and non heterogeneous tumor sizes of the liver. The liver tumor is a grievous disease and needs superior treatment in the initial stages to rescue human life. So, in this study an automated Liver Tumor Segmentation architecture with U-net ResNeXt-50 is proposed which uses LiTS17 dataset that contains 130 abdominal CT images. The proposed architecture follows preprocessing steps including augmentation, windowing, conversion format, and normalization. Followed by the U-Net-ResNeXt-50 architecture to segment out the liver and the tumor. At high level U-Net has the encoder-decoder architecture, where the encoder uses the pre-trained network (ResNeXt-50) and decoder segments out the tumor part of the liver. The proposed model achieved performance accuracy of 99.86 and 90.29 F1-score respectively.

Keywords: Deep learning; CNN; Image segmentations; Pre-trained network; LiTS dataset; U-Net; ResNext-50.

1. INTRODUCTION

The rate of liver tumor spreading in men is almost double that in woman [16]. Typical liver cancer variations include HCC i.e. hepatocellular carcinoma(HCC) that affects the liver majorly due to hepatitis B, C and D. Second, bile duct cancer, which occurs at intersection of the liver, intestine, and gallbladder [23]. Therefore, a thorough diagnosis of tumors in the early stages of the liver is crucial to saving a life. The remedies include blood tests and image detections. India is the third largest country to diagnose deadly diseases, i.e. cancer. The liver tumor detection in males than females is in a ratio of 4:1 approximately [22]. Therefore, early diagnosis is crucial as the 36% survival rate of the patient increases. The survival rate is further decreased, to 13% if the neighboring nodes are affected then reduced to 3% when organ spreading is taking place.

There are various techniques to detect liver diseases such as ultrasound scans, MRI scans, CT scans and biopsy reports etc. MRI scans i.e. medical resonance Imaging tends to have more picture quality of all, but the CT scans are faster to analyze human body parts. Hence, CT scans are used more by radiologists to analyze any disease rapidly. These scans aids in not only identifying diseases but are also used during medical therapy. Applications are applied for detecting good health of the organs like knee, brain, kidney, lung, shoulder, and liver etc. Any kind of tumor detection can be possible with the help of CT scans [24].

Deep learning has shown tremendous outcomes in medical imaging, speech processing, video processing and autonomous vehicles etc. It is a branch of machine learning that uses neural network to answer any above applications. It solves complex problems with multi-dimensional data using multi-dimensional neural networks which encompass input layer, hidden layer and output layer [11].

Diverse deep learning algorithm includes CNN, RNN, DBNN, and auto encoders. Convolution neural network aids in computer vision applications like audio video image processing. Recurrent neural networks are used for natural language processing tasks. DBNN are deep belief neural networks applied to extract outcomes from complex data. Encoders manipulate the input information and decoders extract the input information back in auto encoders.

Hand crafted features are very useful when the training size of the data is very small [15]. For sizable training dataset hand crafted features are not a good choice as it takes more computational time hence CNN directly extracts the features. CNN are made up of convolution layer, pooling layer and fully connected layer. Convolution layer creates various feature maps

of the image using kernel or filter and input image. Pooling layer down samples the data using, methods known as average or max pooling to get dimensionality reduction. Fully connected layer is responsible for classifying outcomes into differential classes.

Image segmentation splits the image into chunks and each chunk implies an object. This technique is applied to tasks like objection detection and recognition. It allocates tags to pixels in the image and the group of each matching pixel is labeled as image segment. Some applications are medical imaging, facial detection and video processing etc. Medical image segmentation helps to find out the uncertainty in any organ of the human body. CT scans are used to analyze this 2D or 3D image data of any organ manually which results in mundane work. Hence, machine learning or deep learning assists doctors to extract data from medical images. Medical imaging performs two crucial tasks i.e. formation of bounding boxes near abnormalities and second is designating the tumors into classes [14].

Previously trained models were handed-down by a new model to perform classification tasks. Basically using input from the dataset's pre-trained model to the new dataset's model. Example, using knowledge of trained building or houses to classify the task of urban or rural regions. This technique is used in applications like audio- video processing, natural language processing etc. Transformed learning paradigm in CNN includes ResNet, GoogleNet, and VGG etc.

U-shaped architecture with encoder decoder network is majorly used in medical image segmentations. This architecture determines what kind of objects that are present in the image and also specifies the locality of the object in the image. The encoder [13] extracts out high level information and decoder up samples the attributes generated at the encoder using skip connection and provides the image mask. Thus, U-Net helps in image segmentations, improvising resolutions and image generations.

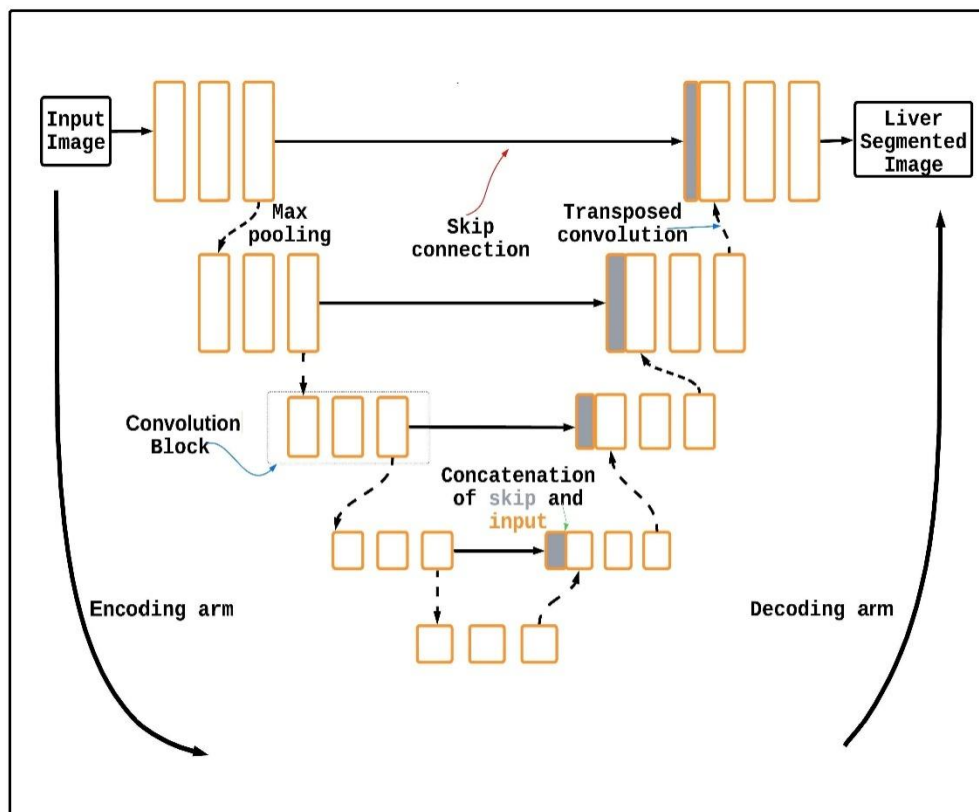


Fig. 1: U-Net Architecture

ResNet [7] stands for residual neural network is a pre-trained network which minimizes the problem of gradient descent. This model generates the concept of skipping layers between neural networks and not letting the gradient to be small.

ResNeXt [8] is the extension of ResNet architecture. It is linked with the concept of group convolutions which incorporates more than one filter and GPUs for increasing efficiency. The group of convolution or cardinality performs split, transform and merge kind of action for the same topology structure to avoid increase in the number of layers and width of neural networks.

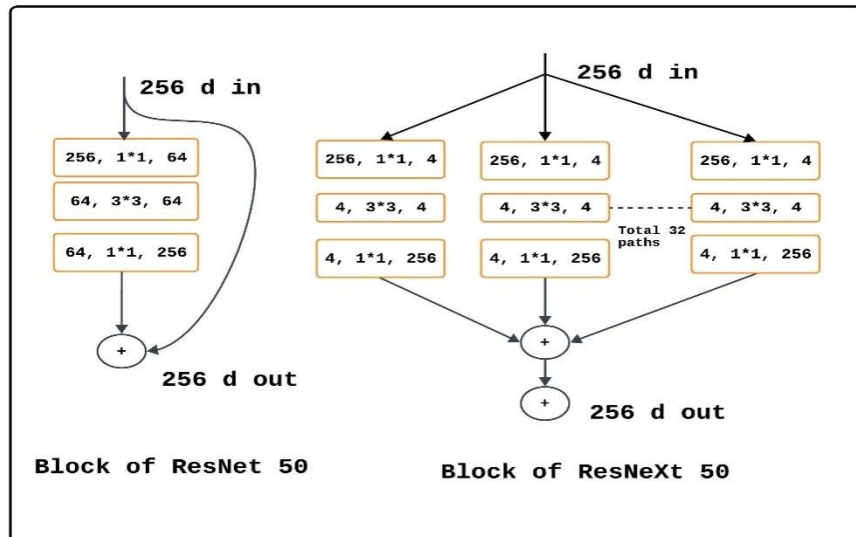


Fig. 2: ResNext-50 Vs ResNeXt-50 model

2. RELATED WORK

The paper employed automatic brain tumor classification using CNN and GoogleNet. Proposed procedure involves 4 steps. Image preprocessing is carried out by doing medium filtering then skull splitting, post processing and classification through GoogleNet. Author applied their procedure on 3 dataset i.e. BRAT2018, BRAT2019, BRAT2020. Highest accuracy was obtained in the BRAT2020 dataset for both segmentation and classification [6].

The author [5] compares 3 algorithms with CNN in segmentation of the liver. The algorithms applied are svm, rfc and adaboost which takes handcrafted features. The CNN algorithm takes automatic features which are more efficient than other algorithms. CNN model here includes 3 convolution layers 2 down sampling layers, a fully connected layer and a softmax classifier at the end. The paper compares hand crafted features with automatic features extraction method for the task of segmentation.

The classification of the covid disease in CT chest scan was presented by the author [3]. The paper achieved the training accuracy of 82.14 % when GoogleNet CNN architecture was applied. System proposed model includes preprocessing steps as conversion of 2D to 3D and binarization. Then applying GoogleNet CNN architecture and classification of covid in the CT chest images were exhibited.

Polyp [1] is the dangerous cancer that can be identified manually or through AI deep learning techniques, when colonoscopy is done. The Kvasir-SEG dataset is used to detect and identify the size and shape of cancer. The author has applied the U-Net-ResNet-50 model to segment out polyps. The U-Net - ResNet architecture uses encoder decoder technique to give away the desired segmentation results. The encoder extracts the features and decoder performs up sampling of the features to get the shape of the tumor. The accuracy and F1-score of the automatic polyp segmentation are 0.9639 and 0.8585.

The researchers [9] proposed a model to indicate building or non building image segmentation tasks. The segmentation task was performed on the aerial image labeling dataset and the carvana dataset. The U-Net architecture with VGG-11 pretrained model was applied on the model both the datasets.

In this paper, we present an introduction in section 1, and study of the research objective in section 2. The new architecture for the objective is described in section 3. The experiment results are represented in section 4. The conclusion and future works are described in section 5.

The key contributions of this paper are mentioned below:

1. Introduced image windowing as part of the pre-processing step to identify the salient regions of the CT scan slice that helps to improve the learning of proposed model.
2. Introduced novel U-Net-ResNeXt-50 architecture for liver tumor segmentation, incorporating a comprehensive preprocessing pipeline that includes data augmentation, image windowing and normalization. This approach enhances the model's performance and generalizability.
3. The proposed model stands out better with dice coefficient of 90.29 as compared with other known state of the art

models.

3. PROPOSED MODEL

The flow of the proposed model is shown in Figure 4. In general terms, the proposed model uses the LitS17 dataset from which the images are loaded and mapped with the segmentation mask using CT mapper. Later, the image data goes from comprehensive pre-processing steps including extracting pixel data, rotating images, image windowing, conversion and normalization. Furthermore, data block generator consisting of data transformation phase that segregates the data into training and validation sets with 70-30 split. Then the generated training data is further injected to the unet-resnext50 model to produce trained prediction engine. The engine is capable to segment out the liver. The predication engine is further evaluated for its generalization using training and validation set data. Below, subsections from describes proposed model in detail.

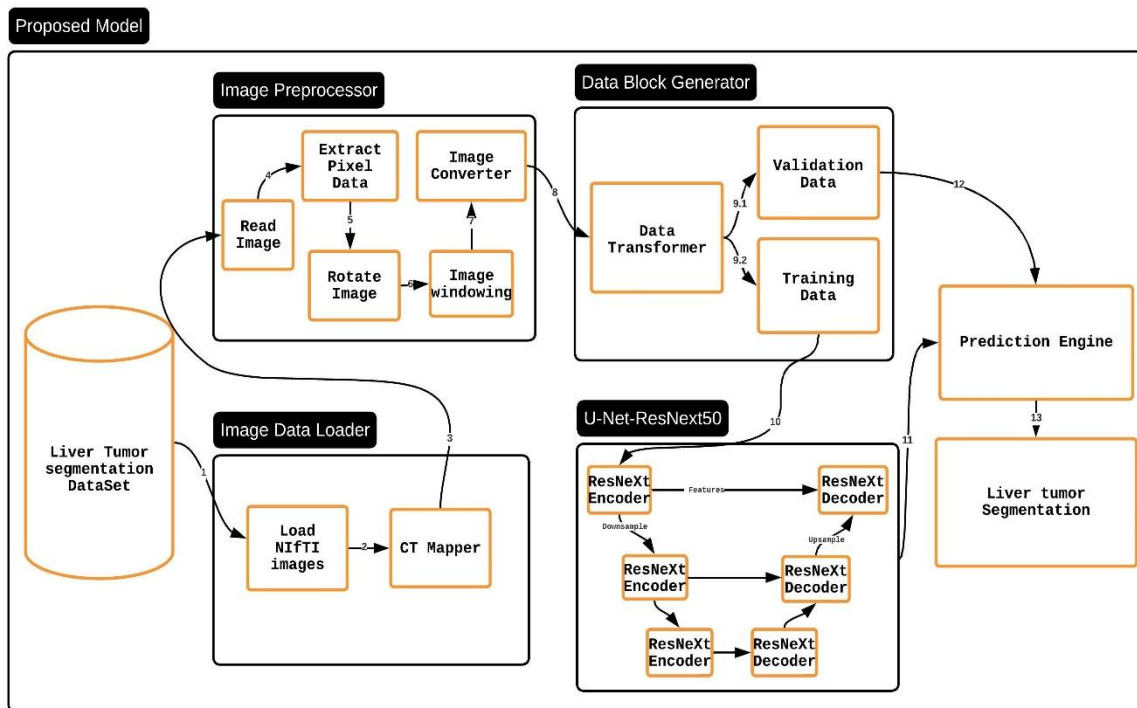


Fig. 3: Proposed model

3.1 Dataset

Liver tumor segmentation (LiTS-2017) is a dataset which is widely used for liver tumor analysis covering non homogeneous tumors of any size and also tumors of irrespective locations. LiTS consists of 130 images. The images are of .nii format. 130 images have a total of 67072 slices [17]. Each image has its segmentation mask of the liver and tumor, which is assumed to be label. These slices are of size 512 & 512. The main aim of using the dataset is that these are CT scan images and give a quick analysis for radiologists or health care workers.

3.2 Image Data Loader

- **Load NIFTI images**

Access of the CT scan sliced image data from the dataset.

- **CT mapper**

CT mapper maps or concatenates the scan image with mask image data.

3.3 Data preprocessing

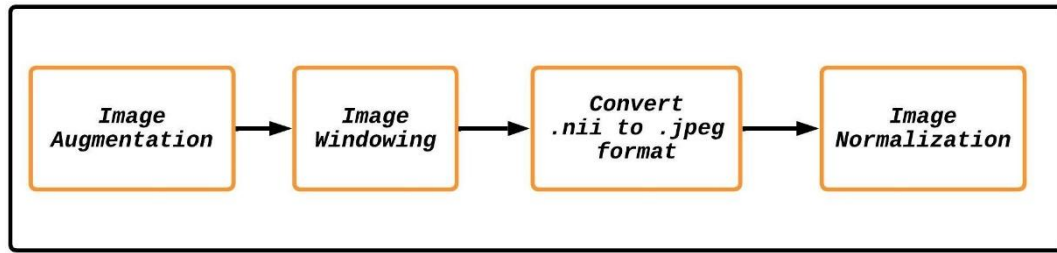


Fig. 4: Proposed model pre-processing steps

- **Data Augmentation**

This step creates variation in training data using image rotation (90 degree), skewing, zooming etc [19]. The consequences of data augmentation are a universal model, reducing over fitting, increase in data samples, and efficiency in performance.

- **Image Windowing**

This step includes adjusting of brightness and contrasts to focus on some parts of the organ with the help of window width and level values. i.e., the window width and level values for the liver have range of 100 to 150 HU and 40 to 60 HU [20]. The values can be determined using the max and min formulas as stated below.

$$\text{Max} = \text{Window Level} + \frac{\text{Window Width}}{2} \quad (1)$$

$$\text{Min} = \text{Window Level} - \frac{\text{Window Width}}{2} \quad (2)$$

- **Normalization**

Normalization modifies the pixel intensity values for standardizing the like-mindedness among a variety of sample image data [4].

3.4 Data block generator

- **Training data**

91 training images with total 23745 slices are trained on UNET-ResNeXt model

- **Validation data**

39 testing images are validated using Prediction engine.

3.5 U-Net-ResNeXt model

U-Net-ResNeXt follows an encoder decoder fully convolution neural network. Our proposed work presents a novel architecture for liver tumor segmentation using the U-Net-ResNeXt-50 32*4d model where 50 stands for the number of layers in the deep convolution layer and 32 is the number of channels with width size 4. This U-Net architecture is composed of encoder, decoder, and the connecting path between encoder and decoder. The encoder leverages ResNeXt-50, which is a pre-trained network which extracts the high level features and decoder up-samples to get the targeted tumor segment. The skip connection is the bridge between encoder and decoder that saves almost most important information. Figure [5] depicts U-net ResNeXt architecture learning flow.

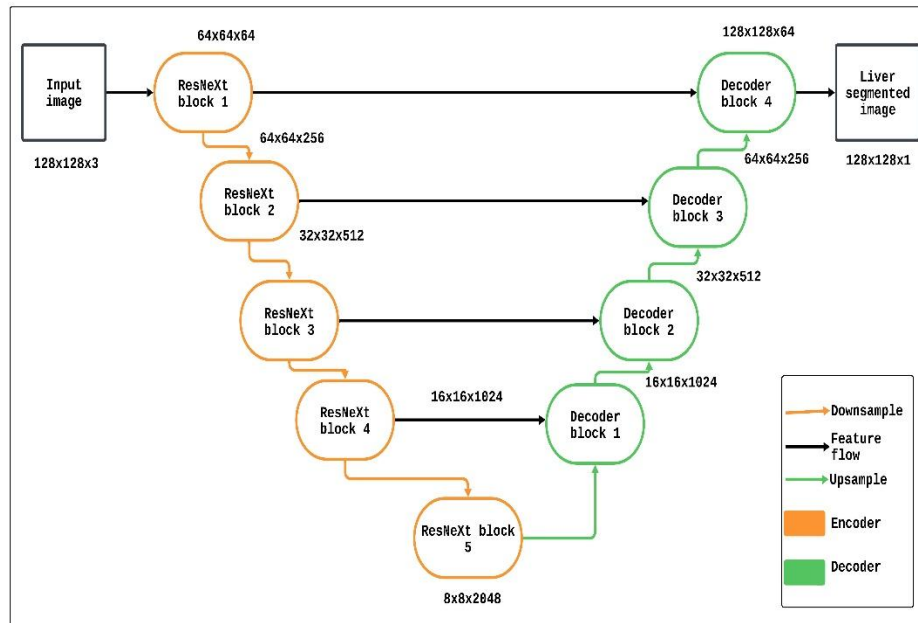


Fig. 5: Proposed model pre-processing steps

4. RESULT ANALYSIS

We used the LiTS dataset to perform the liver tumor segmentation task. The data set is divided into training and validation set containing (91, 39) nii images, respectively. During the training phase, each alternative slice of the training nii image is taken, which totals to 23475 slices with their respective masks. Then U-Net-ResNeXt model was fed with training slices along with training mask. So, the trained model was able to find accurate liver segmentation results.

The trained model is then fed with 130 .nii images that include training and validation images. From each of the .nii images, 3 candidate slices were taken along with mask to assess the segmentation accuracy and compared against the true values [2] from figure [8].

Below table [1-3] shows training accuracy, confusion matrix, precision, recall, and F-1 score related to the performance metrics of the model generated using true values [2] from figure [8]. Figure [6], depicts learning accuracy as number of epochs increases, but after epoch 4 accuracy remains the same. At the same time, figure [7] shows that the training loss is decreasing as the number of epochs are increased. The X-axis illustrates the number of epochs and the Y-axis indicates loss or accuracy. These graphs, are expressed to understand whether data is under-fitted or over-fitted on the training data set.

The figures [9-10] are train and test images generated from the LiTS dataset when the U-Net-ResNeXt model was applied. Thus, the model conveys the best results, when compared to other research papers. The below graph [7] shows paper serial numbers vs performance metrics obtained. These performance metrics can be accuracy, dice coefficient, etc., that are specified in table [2].

Table 1: Training accuracy over epoch

| Epoch | Train loss | Accuracy |
|-------|------------|----------|
| 0 | 0.0082 | 0.9967 |
| 1 | 0.0060 | 0.9980 |
| 2 | 0.0043 | 0.9984 |
| 2 | 0.0032 | 0.9986 |
| 2 | 0.0032 | 0.9986 |

Table 2: Confusion Matrix

| | Predicted Positive | Predicted Negative |
|-----------------|--------------------|--------------------|
| Actual Positive | 79 | 6 |
| Actual Negative | 11 | 34 |

Table 3: Performance Metrics

| Precision | Recall | F1-Score |
|-----------|--------|----------|
| 87.78 | 92.94 | 90.29 |

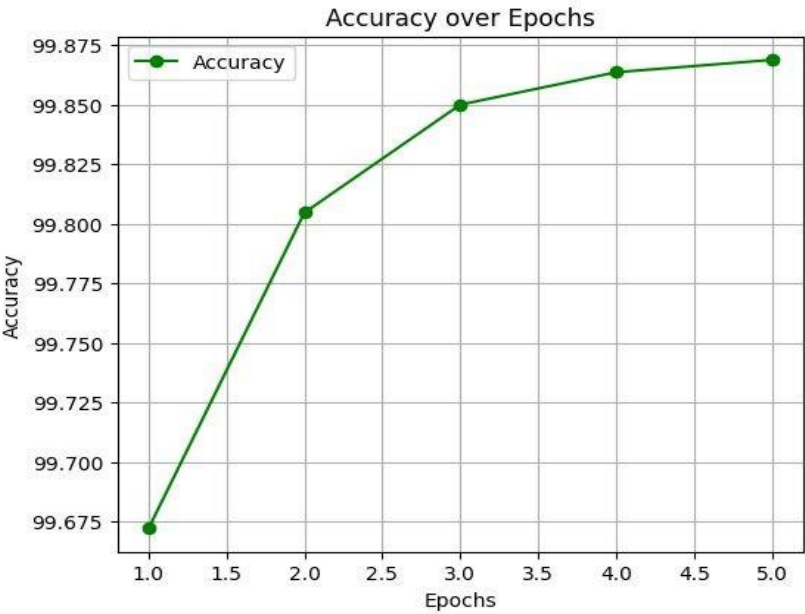


Fig. 6: Accuracy vs Epoch curve



Fig. 7: Loss vs Epoch curve

| Volume# | Radiologist Label | Volume# | Radiologist Label | Volume# | Radiologist Label | Volume# | Radiologist Label | Volume# | Radiologist Label |
|---------|-------------------|---------|-------------------|---------|-------------------|---------|-------------------|---------|-------------------|
| 1 | malignant | 27 | malignant | 53 | malignant | 79 | malignant | 105 | benign |
| 2 | malignant | 28 | malignant | 54 | Normal | 80 | malignant | 106 | benign |
| 3 | malignant | 29 | malignant | 55 | malignant | 81 | malignant | 107 | malignant |
| 4 | malignant | 30 | malignant | 56 | malignant | 82 | benign | 108 | malignant |
| 5 | malignant | 31 | malignant | 57 | benign | 83 | malignant | 109 | malignant |
| 6 | benign | 32 | malignant | 58 | benign | 84 | malignant | 110 | benign |
| 7 | malignant | 33 | Normal | 59 | malignant | 85 | benign | 111 | malignant |
| 8 | malignant | 34 | malignant | 60 | benign | 86 | benign | 112 | benign |
| 9 | malignant | 35 | benign | 61 | malignant | 87 | malignant | 113 | benign |
| 10 | malignant | 36 | malignant | 62 | benign | 88 | benign | 114 | malignant |
| 11 | malignant | 37 | malignant | 63 | benign | 89 | malignant | 115 | malignant |
| 12 | malignant | 38 | malignant | 64 | benign | 90 | benign | 116 | malignant |
| 13 | benign | 39 | Normal | 65 | malignant | 91 | benign | 117 | benign |
| 14 | malignant | 40 | malignant | 66 | benign | 92 | malignant | 118 | malignant |
| 15 | malignant | 41 | malignant | 67 | malignant | 93 | malignant | 119 | malignant |
| 16 | benign | 42 | benign | 68 | malignant | 94 | malignant | 120 | malignant |
| 17 | malignant | 43 | benign | 69 | malignant | 95 | malignant | 121 | benign |
| 18 | malignant | 44 | benign | 70 | malignant | 96 | malignant | 122 | benign |
| 19 | malignant | 45 | benign | 71 | malignant | 97 | malignant | 123 | benign |
| 20 | malignant | 46 | malignant | 72 | benign | 98 | benign | 124 | malignant |
| 21 | malignant | 47 | malignant | 73 | benign | 99 | malignant | 125 | malignant |
| 22 | malignant | 48 | benign | 74 | malignant | 100 | malignant | 126 | malignant |
| 23 | malignant | 49 | malignant | 75 | malignant | 101 | malignant | 127 | benign |
| 24 | malignant | 50 | malignant | 76 | malignant | 102 | malignant | 128 | benign |
| 25 | benign | 51 | benign | 77 | benign | 103 | malignant | 129 | malignant |
| 26 | Normal | 52 | malignant | 78 | malignant | 104 | benign | 130 | malignant |

Fig. 8: LiTS17 Dataset Ground Truth

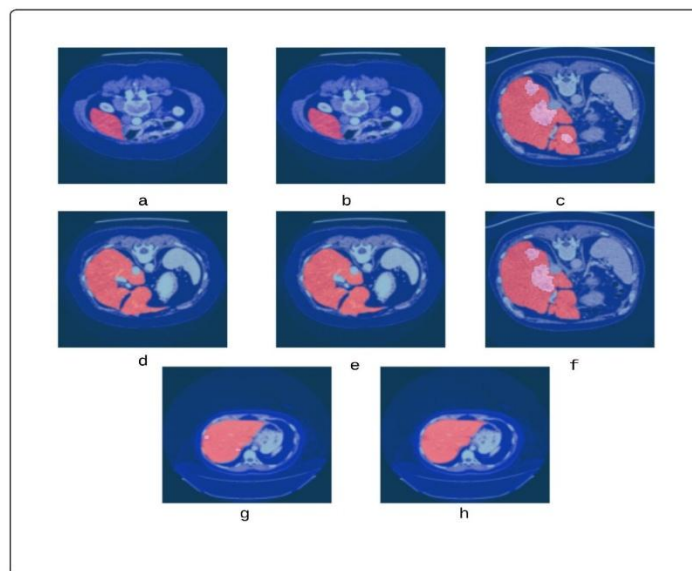


Fig. 9: Trained Results with U-Net ResNeXt

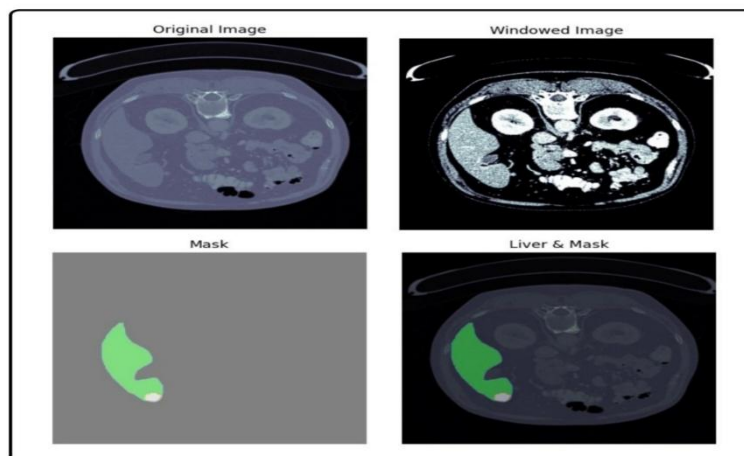


Fig. 10: Test Result with U-Net ResNext

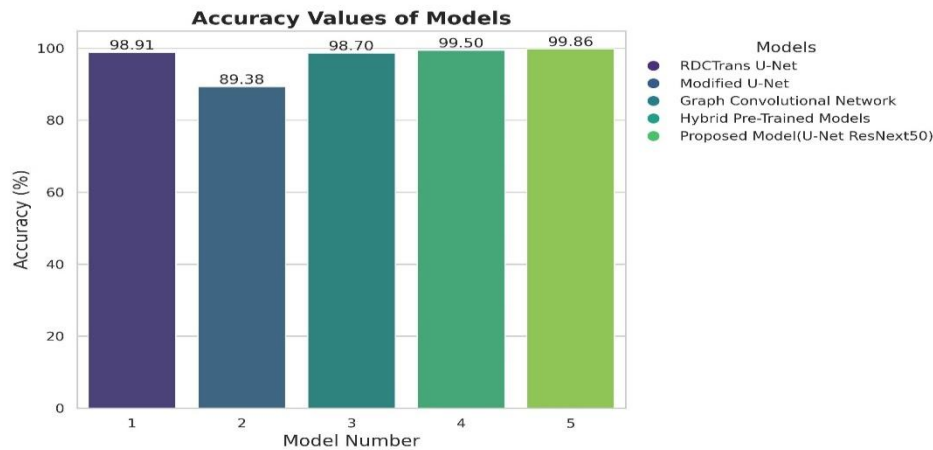


Fig. 11: Paper serial numbers vs Performance metric

| No | Dataset | Findings | LIVER Acc | Tumo Acc) |
|----------------|----------------|---|-------------|---------------------------------------|
| [12] | LiTS | ResNext-50 along with dilated convolution and transformer were used as encoders in liver tumor segmentation using a U-Net based network (RDCTrans U-Net). | 93.38(Dice) | 98.91(Acc), 89.87(Dice) |
| [18] | LiTS, 3DIRCADb | Modified U-Net was applied on both 2D and 3D liver tumor dataset. Image resize was performed with modified U-Net on training dataset. Dice similarity was measured to analyze the performance of the model. | 96.15(Dice) | 89.38(Dice) |
| [10] | LiTS | Liver tumor segmentation with help of graph convolutional network was carried out. The proposed method uses image processing, and graph embedding with simple linear iterative clustering. Then, preparing a neural network graph model and lastly training and testing was performed on the created model. | 99.1(Acc) | 98.7(Acc) |
| [21] | LiTS, 3DIRCADb | Data augmentation was performed as a preprocessing step. Two methods were applied to train the model including (Deep Lab V3 + ResNet-50) and second model consisting of (VGG 16+ ResNet-50+ U-Net+LSTM). | | 99.5(model1 acc), 99.1(model2 acc) |
| Proposed Model | LiTS | Data augmentation, image windowing, conversion to .jpeg and normalization are performed as preprocessing steps. The U-Net-ResNeXt-50-32*4d model is applied on the trained data and the accuracy results obtained are significant. | | 99.86(Acc), 90.29(Dice) |

Table 4: Comparing obtained results with other models and datasets

5. CONCLUSION

We aim to detect tumors in the liver organ with the help of the U-Net-ResNeXt-50 model. The accuracy and dice coefficient obtained by the model are 99.86 and 90.29 respectively. This model could be used by healthcare workers, especially radiologists, to detect liver tumors on CT images. In future work, we wish to apply the model to a 3D image dataset. We also want to detect non-homogeneous tumors with a larger number of training and testing image data in real-time image analysis.

REFERENCES

- [1] Saruar Alam et al. "Automatic polyp segmentation using u-net-resnet50". In: *arXiv preprint arXiv:2012.15247* (2020).
- [2] Khaled Alawneh et al. "LiverNet: diagnosis of liver tumors in human CT images". In: *Applied Sciences* 12.11

- (2022), p. 5501.
- [3] Nesreen Alsharman and Ibrahim Jawarneh. "GoogleNet CNN neural network towards chest CT-coronavirus medical image classification". In: *J. Comput. Sci* 16.5 (2020), pp. 620–625.
 - [4] Pierre-Luc Delisle et al. "Realistic image normalization for multi-domain segmentation". In: *Medical Image Analysis* 74 (2021), p. 102191.
 - [5] Anand Deshpande, Vania V Estrela, and Prashant Patavardhan. "The DCT- CNN-ResNet50 architecture to classify brain tumors with super-resolution, convolutional neural network, and the ResNet50". In: *Neuroscience Informatics* 1.4 (2021), p. 100013.
 - [6] Sahar Gull, Shahzad Akbar, and Habib Ullah Khan. "Automated detection of brain tumor through magnetic resonance images using convolutional neural network". In: *BioMed Research International* 2021.1 (2021), p. 3365043.
 - [7] Kaiming He et al. "Deep residual learning for image recognition". In: *Proceedings of the IEEE conference on computer vision and pattern recognition*. 2016, pp. 770–778.
 - [8] Saifuddin Hitawala. "Evaluating resnext model architecture for image classification". In: *arXiv preprint arXiv:1805.08700* (2018).
 - [9] Vladimir Iglovikov and Alexey Shvets. "Ternausnet: U-net with vgg11 encoder pre-trained on imagenet for image segmentation". In: *arXiv preprint arXiv:1801.05746* (2018).
 - [10] Maryam Khoshkhabar et al. "Automatic Liver Tumor Segmentation from CT Images Using Graph Convolutional Network". In: *Sensors* 23.17 (2023), p. 7561.
 - [11] Vaibhav Kumar and ML Garg. "Deep Learning as a Frontier of Machine Learning: A". In: *International Journal of Computer Applications* 975 (2018), p. 8887.
 - [12] Lingyun Li and Hongbing Ma. "Rdctrans u-net: A hybrid variable architecture for liver ct image segmentation". In: *Sensors* 22.7 (2022), p. 2452.
 - [13] Xiaojin Li et al. "Image segmentation based on improved unet". In: *Journal of Physics: Conference Series*. Vol. 1815. 1. IOP Publishing. 2021, p. 012018.
 - [14] Haofu Liao, S Kevin Zhou, and Jiebo Luo. *Deep network design for medical image computing: principles and applications*. Academic Press, 2022.
 - [15] Wenyi Lin et al. "Comparison of handcrafted features and convolutional neural networks for liver MR image adequacy assessment". In: *Scientific Reports* 10.1 (2020), p. 20336.
 - [16] Chun-Yu Liu, Kuen-Feng Chen, and Pei-Jer Chen. "Treatment of liver cancer". In: *Cold Spring Harbor perspectives in medicine* 5.9 (2015), a021535.
 - [17] Shunyao Luan et al. "Adaptive attention convolutional neural network for liver tumor segmentation". In: *Frontiers in Oncology* 11 (2021), p. 680807.
 - [18] RV Manjunath and Karibasappa Kwadiki. "Modified U-NET on CT images for automatic segmentation of liver and its tumor". In: *Biomedical Engineering Advances* 4 (2022), p. 100043.
 - [19] Agnieszka Mikołajczyk and Michał Grochowski. "Data augmentation for improving deep learning in image classification problem". In: *2018 international interdisciplinary PhD workshop (IIPhDW)*. IEEE. 2018, pp. 117–122.
 - [20] Kube J Murphy A Baba Y. "Windowing CT". In: *Radiopaedia.org* (2017).
 - [21] Esam Othman et al. "Automatic detection of liver cancer using hybrid pre-trained models". In: *Sensors* 22.14 (2022), p. 5429.
 - [22] Krishnan Sathishkumar et al. "Cancer incidence estimates for 2022 & projection for 2025: result from National Cancer Registry Programme, India". In: *Indian Journal of Medical Research* 156.4&5 (2022), pp. 598–607.
 - [23] Kazuaki Takabe and Matthew GK Benesch. "Types of Cancer and Research Covered in World Journal of Oncology". In: *World Journal of Oncology* 13.6 (2022), p. 325.
 - [24] Jeyaprakash Vasanth Wason and Ayyappan Nagarajan. "Image processing techniques for analyzing CT scan images towards the early detection of lung cancer". In: *Bioinformation* 15.8 (2019), p. 596.